Poulton et al., https://doi.org/10.1083/jcb.201607022

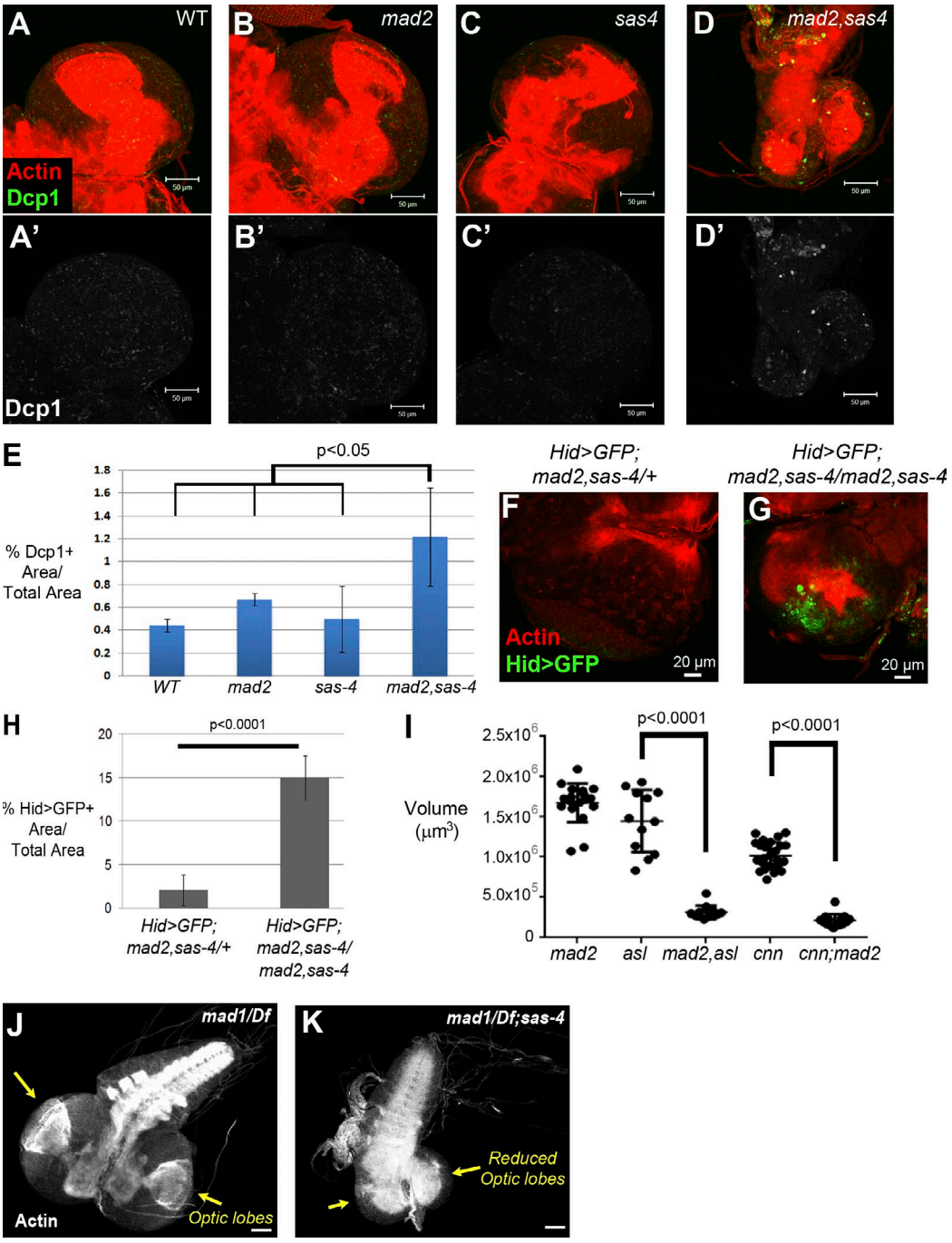

Figure S1. **Increased apoptosis and reduced brain size in multiple genotypes eliminating centrosomes and the SAC.** (A–E) As we observed by using Casp3 to mark apoptosis (Fig. 1), the percentage of cells expressing high levels of the effector caspase Dcp1 (green; Florentin and Arama, 2012) was also significantly elevated in *mad2 sas-4* brains relative to WT or single mutants. A–D are maximum-intensity projections. Phalloidin in red reveals the brain neuropil. A′–D′ show Dcp1 staining. (F–H) Consistent with this, expression of the proapoptotic protein Hid, assayed by a Hid>GFP reporter (Tanaka-Matakatsu et al., 2009), was significantly elevated in *mad2 sas-4* mutants (G), but not in control animals (heterozygotes over the TM6b balancer, F; quantified in H). Hid>GFP expression was not examined for single mutants. F and G are single confocal sections. Phalloidin is in red. (I) Consistent with our findings in *mad2 sas-4* brains, simultaneously eliminating the SAC and centrosomes in *mad2* double mutants with *asl* or *cnn* resulted in significantly smaller late third instar brain size (6 d AEL). Error bars represent means ± SD. (J and K) Representative images (phalloidin) illustrate the reduced brain size of late third instar *mad1/Df;sas-4* double mutants relative to *mad1* single mutants (quantification is in Fig.1 K). Bars, 50 µm.

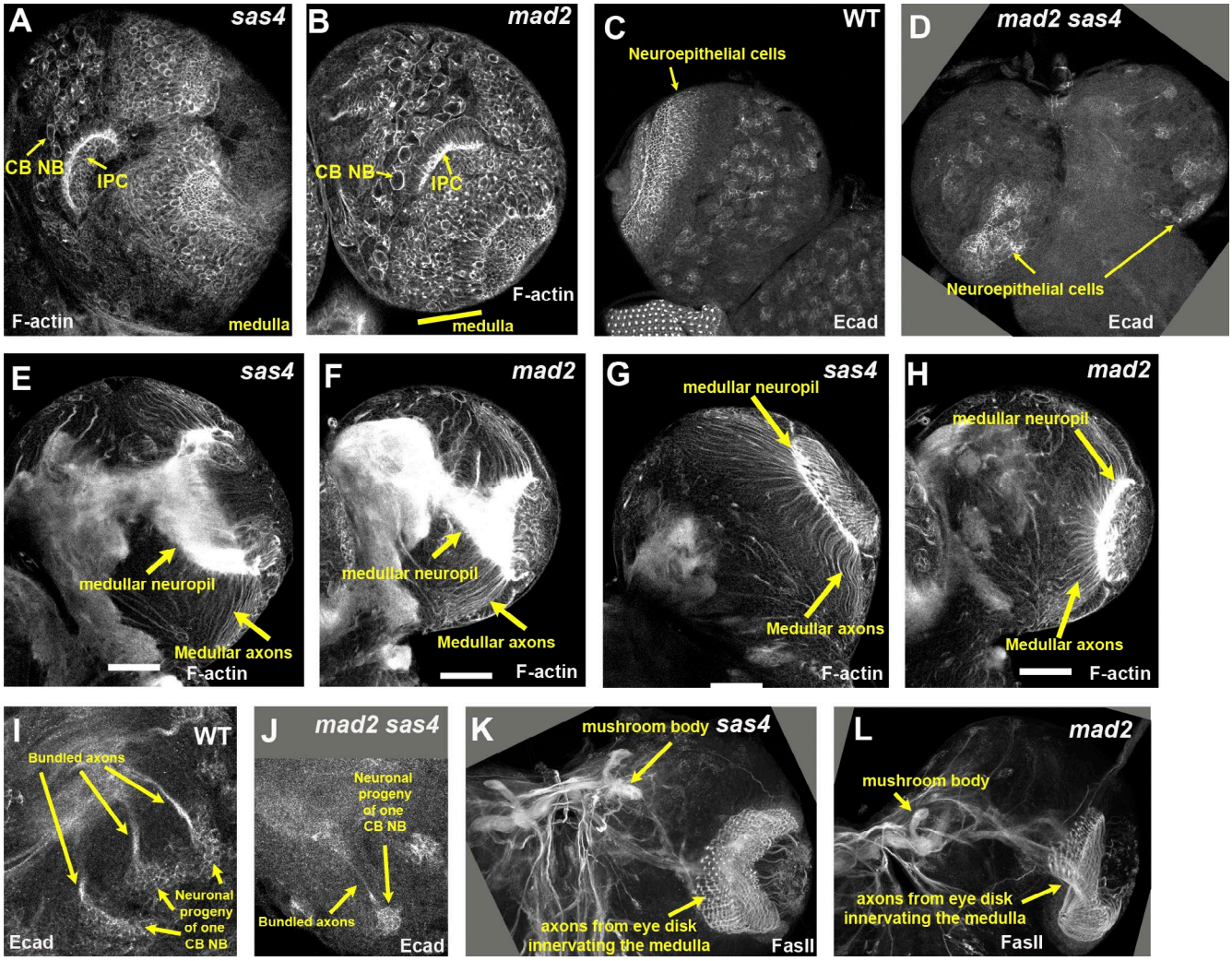

Figure S2. **Further analysis of brain architecture in single and double mutants.** (A and B) Posterior views of third instar larva. F-actin staining revealed normal architecture in *sas-4* and *mad2* single mutants (compare with Fig. 2 N). IPC, inner proliferative center. (C and D) Ecad-labeled neuroepithelial cells of the WT medulla (C), which were highly disorganized in *mad2 sas-4* double mutants (D). (E–H) F-actin staining also highlights the axons from medullar neurons that extended into the medullar neuropil. These structures were normal in *sas-4* and *mad2* single mutants (compare with Fig. 2, P and S). (I) Progeny of individual WT CB NBs sent bundled axons that labeled with Ecad. (J) *mad2 sas-4* double mutant CB NBs retained this ability. (K and L) FasII labeled the mushroom body as well as incoming axons from the eye disc photoreceptors. Both were present and overtly normal in *sas-4* and *mad2* single mutants (compare with Fig. 2 U).

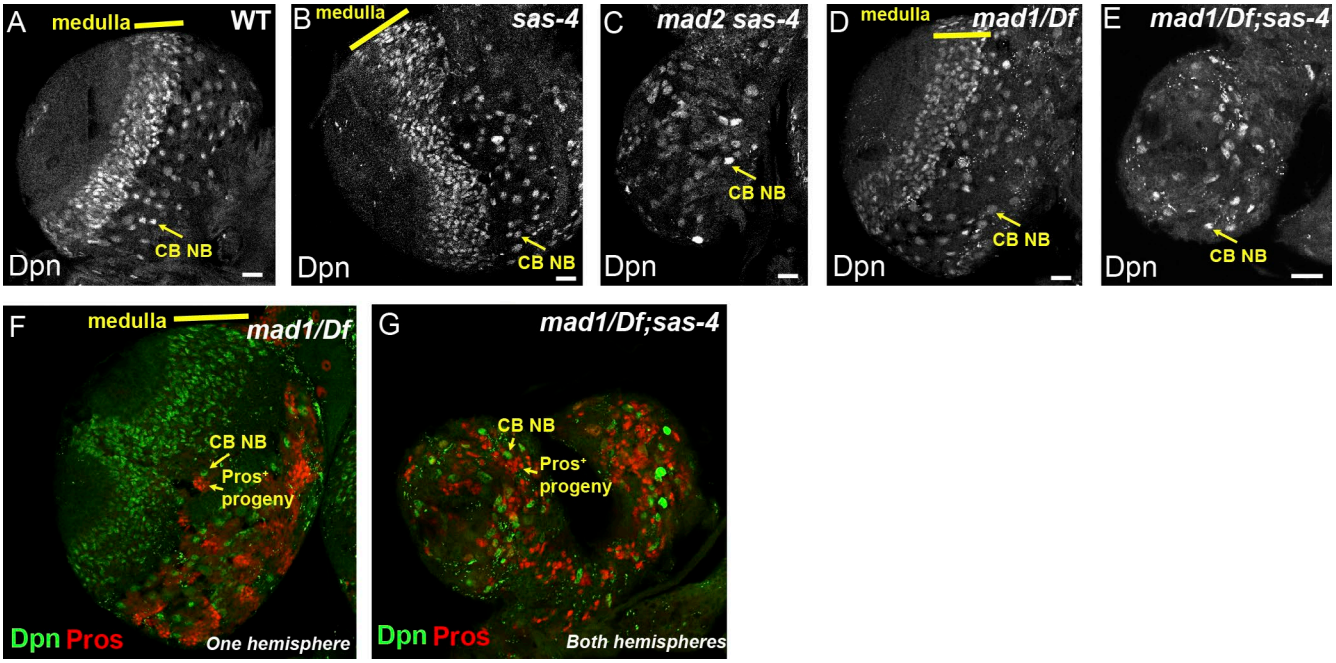

Figure S3. ***mad1 sas-4*double mutants phenocopy the *mad2 sas-4* brain development defects.** (A–E) Late third instar brains stained for the NB marker Dpn. WT (A) and each of the single mutants (B and D) had a normal CB region and a band of medullary NBs in the optic lobe. However, in *mad2 sas-4* (C) or *mad1/Df;sas-4* (E) double mutants, the medulla was reduced or lost, and the remaining CB NBs were highly disorganized. (F and G) Late third instar brains stained for the NB marker Dpn and the marker of their progeny Pros. The normal band of medullar NBs seen in *mad1/Df* single mutants (F) is absent in *mad1/Df;sas-4* double mutants (G), but in both genotypes, CB NBs were associated with groups of Pros$^+$ progeny. Bars, 20 µm.

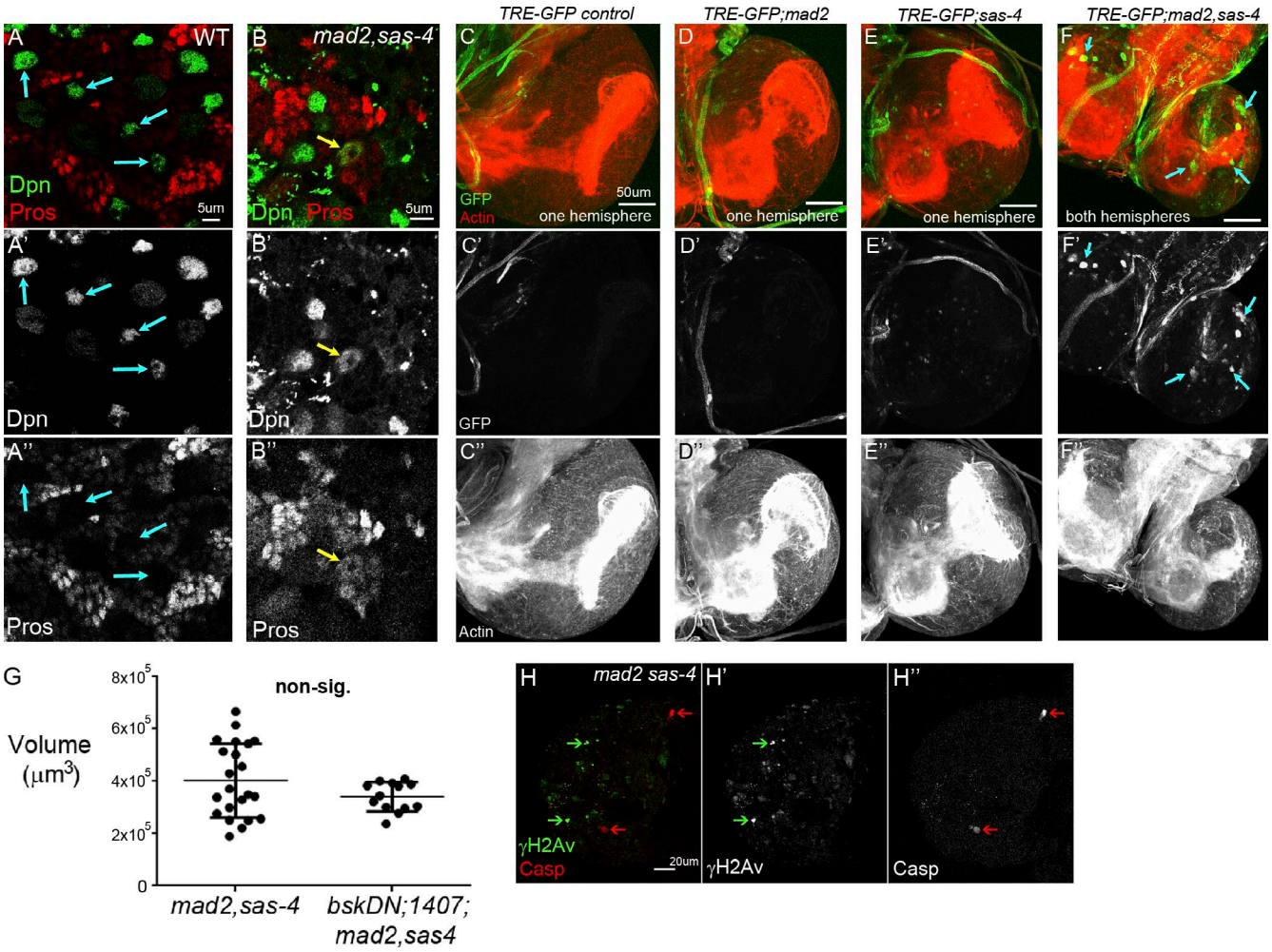

Figure S4. **Defective differentiation and elevated JNK signaling in *mad2 sas-4* brains.** (A and B) NBs, as stem/progenitor cells, normally divide asymmetrically, with one daughter retaining stem cell fate and one going down a differentiation route to become a ganglion mother cell. To test the hypothesis that *mad2 sas-4* NBs are prone to defective differentiation, as was observed previously in NBs with excess centrosomes and lacking the SAC (Gogendeau et al., 2015), we costained for the CB NB marker Dpn (green) along with Pros (red), a marker of CB NB progeny. Dpn was nuclear in WT NBs (A, arrows), whereas Pros asymmetrically localized to a basal cortical crescent and then segregated into ganglion mother cells, where it moved to the nuclei to regulate gene expression, which promotes differentiation and cell cycle exit (the Pros cortical crescent in CB NBs is difficult to visualize, particularly during interphase, relative to the strong nuclear signal of adjacent progeny; Yu et al., 2006). Thus, in WT NBs, Dpn and Pros were not found together in the nucleus (0/224 NBs from seven hemispheres; Gogendeau et al., 2015). However, consistent with defective differentiation in *mad2 sas-4* CB NBs, we observed a modest but significant incidence of colocalization of Dpn and Pros in CB nuclei (B, arrows; 2.7%; 6/223 NBs from 17 hemispheres). A′ and B′ show the Dpn channel only, labeling NBs; A′′ and B′′ show the Pros channel only, marking NB progeny. (C–F) To analyze levels of JNK activity in brain cells, we crossed the JNK reporter TRE-GFP (Chatterjee and Bohmann, 2012) into the relevant mutants. In WT, *mad2*, or *sas-4* single mutant brains, there was no strong expression of GFP (green) in cells of the CB or optic lobes, indicating low levels of JNK activity. Note that in all genotypes, there was a fairly strong GFP signal in the large bundled neurons emanating from the brain but separate from the lobe proper. However, in *mad2 sas-4* brains (F), many cells in the brain lobes displayed very high levels of JNK activity (F′, arrows). C′–F′ show the GFP channel only, indicating TRE-GFP expression; C′′–F′′ show the actin channel, which marks overall brain architecture and neuropils. All samples were imaged on the same day using the same microscope settings, and images were adjusted equally. Images shown are maximum-intensity projections of z stacks encompassing the entire brain lobe. (G) Despite the high levels of JNK activity, inhibiting JNK activity did not lead to any increase in the size of *mad2 sas-4* brains. Because blocking apoptosis by p35 expression did lead to increased *mad2 sas-4* brain size (Fig. 3 G), this suggests that JNK is likely not a key mediator of apoptosis in double mutant brains. Error bars represent means ± SD. (H) Costaining *mad2 sas-4* brains for the apoptotic marker Casp (red arrows) and the DNA damage marker γ-H2Av (green arrows) revealed that many of the cells that express one marker did not also express the other. H′ shows γ-H2Av marked cells with DNA damage; H′′ shows the Casp channel only, labeling dying cells.

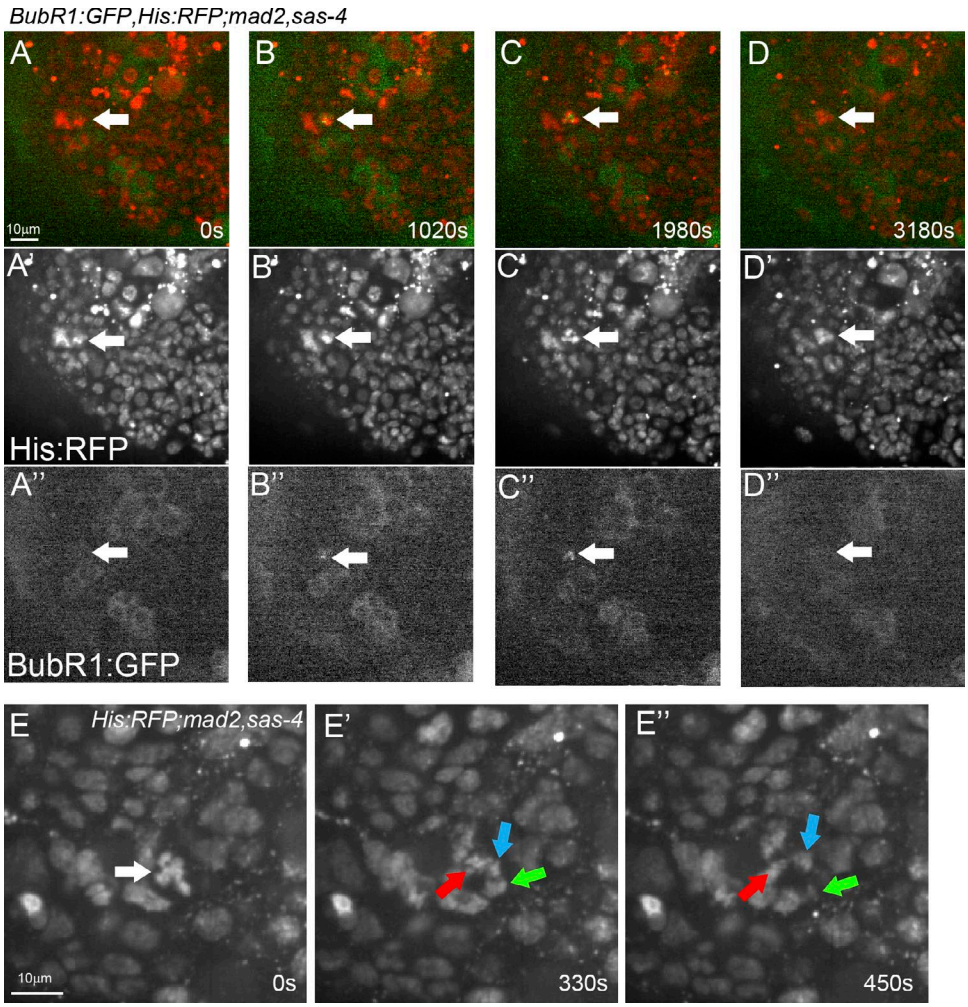

Figure S5. **Examples of severe mitotic errors in *mad2 sas-4* brains.** (A–D) Still images from separate time points of Video 4 showing a failed attempt at mitosis in a *mad2 sas-4* double mutant brain expressing His:RFP and BubR1:GFP. The condensed chromatin of the relevant nucleus is visible at time point zero (A). Then, BubR1:GFP began to accumulate at kinetochores (B). Higher levels of BubR1 accumulated, and although much time had passed, no attempt at anaphase occurred (C). Eventually, BubR1 signal faded and the chromatin decondensed without any chromosome segregation (D). Arrows track a single cell undergoing a failed mitotic division. A′–D′ show the His:RFP channel only, labeling all nuclei; A′′–D′′ show the BubR1:GFP channel only, revealing a transient accumulation of BubR1 on a cell attempting mitosis. (E–E′′) Still images (Video 5) of His:RFP expression in a *mad2 sas-4* mutant brain reveal a tripolar division. Each daughter nucleus is marked by a different color arrow.

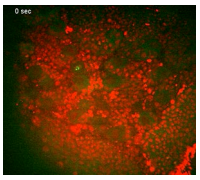

Video 1. **WT brains are highly proliferative.** Representative WT late third instar brain expressing His:RFP and BubR1:GFP. His :RFP labels all nuclei. BubR1:GFP rapidly accumulates on kinetochores during prometaphase immediately after NEB. In WT, many nuclei undergo mitosis in the time frame of a single video. Quantification of the time from NEB to anaphase onset is shown in Fig. 5 I. Images were acquired every 30 s. Video is displayed at 13 frames per second.

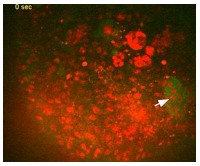

Video 2. ***mad2 sas-4* mutant brains have dramatically fewer dividing cells.** Third instar brain from a *mad2 sas-4* animal expressing His:RFP and BubR1:GFP. The arrow highlights the lone dividing cell present in this brain hemisphere during the course of this video. The reduced mitotic index in *mad2 sas-4* brains relative to WT or single mutants is shown in Fig. 2 (F–J). Images were acquired every 30 s. Video is displayed at 13 frames per second.

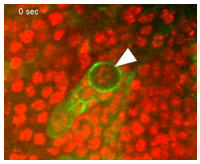

Video 3. **Despite loss of both centrosomes and the SAC, *mad2 sas-4* NBs remain capable of asymmetric division.** Cropped view of a third instar *mad2 sas-4* brain expressing His:RFP and the cortical actin marker Moe:GFP. The arrowhead indicates a mitotic NB that will undergo asymmetric division over the course of the video. Images were acquired every 30 s. Video is displayed at 12 frames per second.

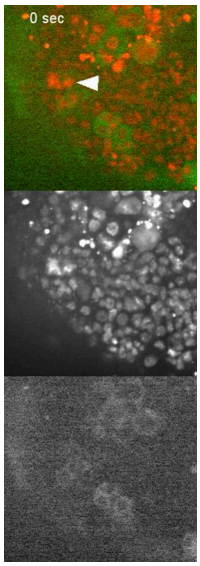

Video 4. **Failed mitosis in *mad2 sas-4* mutant brain.** Third instar brain from a *mad2 sas-4* animal expressing His:RFP and BubR1:GFP. The top panel shows the merge of the middle panel (His:RFP) and bottom panel (BubR1:GFP). The arrowhead indicates a nucleus that appears to attempt mitosis as suggested by the condensed chromatin, and, ∼540 s later in the video, the accumulation of BubR1:GFP suggests NEB has occurred and kinetochores have formed. After spending ∼1,600 s in this state, BubR1:GFP leaves the kinetochores, though no chromosome segregation has occurred (in WT, this portion of mitosis typically lasts only ∼600 s). Subsequently, the chromatin decondenses, indicating mitotic exit. Images were acquired every 30 s. Video is displayed at 12 frames per second.

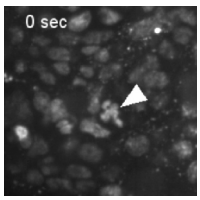

Video 5. **Multipolar division in the *mad2 sas-4* brain.** Cropped view of a third instar *mad2 sas-4* brain expressing His:RFP. The arrowhead highlights a mitotic cell about to undergo mitosis. During anaphase, the chromatin segregates into three distinct daughter nuclei, and each moves separately out of the frame. Images were acquired every 30 s. Video is displayed at five frames per second.

References

Chatterjee, N., and D. Bohmann. 2012. A versatile ΦC31 based reporter system for measuring AP-1 and Nrf2 signaling in *Drosophila* and in tissue culture. *PLoS One.* 7:e34063. http://dx.doi.org/10.1371/journal.pone.0034063

Florentin, A., and E. Arama. 2012. Caspase levels and execution efficiencies determine the apoptotic potential of the cell. *J. Cell Biol.* 196:513–527. http://dx.doi.org/10.1083/jcb.201107133

Gogendeau, D., K. Siudeja, D. Gambarotto, C. Pennetier, A.J. Bardin, and R. Basto. 2015. Aneuploidy causes premature differentiation of neural and intestinal stem cells. *Nat. Commun.* 6:8894. http://dx.doi.org/10.1038/ncomms9894

Tanaka-Matakatsu, M., J. Xu, L. Cheng, and W. Du. 2009. Regulation of apoptosis of *rbf* mutant cells during *Drosophila* development. *Dev. Biol.* 326:347–356. http://dx.doi.org/10.1016/j.ydbio.2008.11.035

Yu, F., C.T. Kuo, and Y.N. Jan. 2006. *Drosophila* neuroblast asymmetric cell division: recent advances and implications for stem cell biology. *Neuron.* 51:13–20. http://dx.doi.org/10.1016/j.neuron.2006.06.016